NRIAG Journal of Astronomy and Geophysics (2015) 4, 256–265

National Research Institute of Astronomy and Geophysics

NRIAG Journal of Astronomy and Geophysics

www.elsevier.com/locate/nrjag

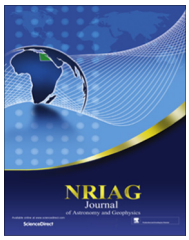

Analytical study of pulsed laser irradiation on some materials used for photovoltaic cells on satellites

Afaf M. Abd El-Hameed

National Research Institute of Astronomy and Geophysics, NRIAG, Helwan, Egypt

Received 13 February 2015; revised 16 August 2015; accepted 21 September 2015
Available online 23 October 2015

KEYWORDS

Pulsed laser;
Si and GaAs;
Heating process;
Temperature;
Analysis

Abstract The present research concerns on the study of laser-powered solar panels used for space applications. A mathematical model representing the laser effects on semiconductors has been developed. The temperature behavior and heat flow on the surface and through a slab has been studied after exposed to nano-second pulsed laser. The model is applied on two different types of common active semiconductor materials that used for photovoltaic cells fabrication as silicon (Si), and gallium arsenide (GaAs). These materials are used for receivers' manufacture for laser beamed power in space. Various values of time are estimated to clarify the heat flow through the material sample and generated under the effects of pulsed laser irradiation. These effects are theoretically studied in order to determine the performance limits of the solar cells when they are powered by laser radiation during the satellite eclipse. Moreover, the obtained results are carried out to optimize conversion efficiency of photovoltaic cells and may be helpful to give more explanation for layout of the light-electricity space systems.

1. Introduction

Laser-based long distance energy transmission technology has concerned the importance from many researchs and institutions including NASA Research Center (Landis, 1991b; Schafer and Gray, 2012). This technology caused the interest of space solar power station builders because they need to find a way to transport the solar energy composed in space to the ground (Landis, 1991a; Flournoy, 2012; Raikunov et al., 2011). The Laser based long-range energy transmission mainly includes two opposite converting processes between electric energy and light energy. The electricity-light conversion process is conducted by electro-pumping laser, while the light-electricity conversion is conducted by photovoltaic cell. During the process of laser beam long-range energy transmission based on the photovoltaic theory, the temperature elevation of the photovoltaic cell under laser irradiation would affect its photoelectric conversion efficiency (Schafer and Gray, 2012; Yuan et al., 2013). The high

E-mail address: afaf_m2000@yahoo.com
Peer review under responsibility of National Research Institute of Astronomy and Geophysics.

ELSEVIER Production and hosting by Elsevier

http://dx.doi.org/10.1016/j.nrjag.2015.09.005

power weight ratio of the photovoltaic cell has always been desire in the applications of spacecraft and satellites; therefore, multilayers and sheets for photovoltaic cells are commonly used in these applications. The type of photovoltaic cells, which have the advantages of small size, high efficiency and a strong capability of resistance to radiation degradation, deserved to be the best choice for practical applications (King et al., 2007; Green et al., 2011).

The temperature of the solar cell would be comparatively high due to the relatively high power density of the Laser beam, and thus would lead to a reduction in its efficiency. In other words, the temperature elevation would reduce the fill factor and further reduce the efficiency of solar cell (Green, 1998; Cuce et al., 2013; Laudani et al., 2013). Moreover, the efficiency loss caused by the temperature elevation may be the main factor influencing the performance of laser based long range energy transmission (Landis, 1991a; Yuan and Wu, 2014). In addition, temperature elevation would develop thermal stress in photovoltaic cells, which in turn would affect cell's efficiency, and might cause physical damage in cell, leading it to be failure (Kuanr et al., 1996; Shuvalov et al., 2002). So, In order to avoid failure of the cell, it is very important to realize the temperature and stress characteristics of the cell under laser irradiation.

In this study, the thermal energy flowing in the cell as a temperature evolution after cell irradiation by pulsed laser is theoretically investigated. A mathematical model, describing the temperature behavior and heat diffusion process is established. The computations are applied on two common materials used for photovoltaic cells manufactures, and the results are analyzed.

2. Theoretical modeling

In material science, laser heating process is an important aspect in laser processing of semiconductor especially in small scale fabrication and technological advance. In laser-material interactions, many processes typically involve moving a target, against a stationary which can be either pulsed or continuous. The intensity of the beam may vary crossways or not, so a model of a moving target may have to account for either a temporally varying intensity as the material meets first the low-intensity leading edge, then the high-intensity middle, and finally the low-intensity trailing edge, or the cumulative effect of a number of pulses of equal intensity. In much of materials research the aim is to determine the effect of laser radiation on some material property and this kind of moving geometry can represent an unnecessary complication. The material is therefore heated statically for a limited time and the intensity is often, but not always, assumed to be constant over this time. These simplifications are often essential in order to make the problem mathematically easy to be solved. In the present study, it is assumed that, with surface absorption and temperature-independent thermo-physical properties such as conductivity, density and heat capacity, it is possible to solve the heat diffusion equations subject to boundary conditions which define the geometry of the sample. For a slab or semi infinite target heated by a laser with a beam much larger in area than the depth affected, corresponding to 1-Dimensional heat diffusion as illustrated in the following figure.

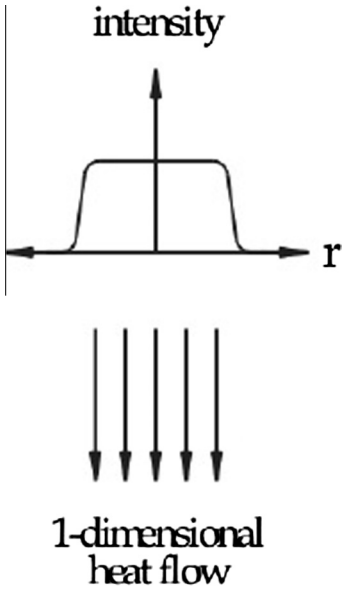

2.1. Material response

The details of the material response will depend on the particular material system and the laser processing conditions. As was mentioned earlier, if laser induced excitation rates are slow compared to the thermalization time, then the process is denoted as photo thermal, and one can consider the absorbed laser energy as being directly transformed into heat. In this case, the material response is a function many factors such as local material heating and cooling rates, maximum temperatures reached, and temperature gradients. All of which can be determined from the solution to the heat equation for the given irradiation conditions. This is may be occurred because of the material heating rates can be so extreme, and reaching as high as 10^9 K/s for nanosecond (ns) pulses (Brown and Arnold, 2010).

2.2. Basic equations

The material response can be explained as a result of elevated temperatures. Therefore, it is important to be able to model the flow of heat inside a material. The temporal and spatial evolutions of the temperature field inside a material are governed by the heat equation. When the material surface is irradiated with a laser, it absorbs the energy. This absorbed optical energy is converted into thermal energy, propagated as heat, and begin to spread on to the cell surface. This thermal energy is responsible for the increase of the temperature in the cell (David Sands, 2011). According to the laws of optics, the laser beam intensity from the source I_0 is transmitted into the surface of the cell with intensity I_T, where

$$I_T = I_0(1 - R) \tag{1}$$

Here R is the reflectivity of the material. The optical intensity will be absorbed inside the material and decays exponentially with depth x according to the Beer–Lambert law formula:

$$I(x) = I_T e^{-\alpha x} \tag{2}$$

$I(x)$ is the transmitted intensity inside the material, and α is the optical absorption coefficient. The heat source, due to the laser irradiation, represents the heat statement $h(x)$, is given as

$$h(x) = -\frac{\partial I(x)}{\partial x} \tag{3}$$

Using formulas in Eqs. (1) and (2), we obtain

$$h(x) = \alpha\, I(x) \;= \alpha\, I_0(1-R)e^{-\alpha x} \tag{4}$$

Eq. (4) represents the heat source contribution, and must be taken into consideration in the equation of the heat propagation.

In heating process, to determine the effect of laser radiation on some material property, the material is therefore heated for a limited time and the intensity is assumed to be constant over this time (David Sands, 2011). The technique of energy conversion and heat flow processes can be mathematically described using the equations of the heat flow and diffusion process. To simplify the solution of the problem, it is considered here that, the thermal parameters are independent of the temperature and the heat flow is in one dimensional with the conduction only in the direction along the depth or thickness x ($0 \leqslant x \leqslant L$), and L is the total thickness of the slab. Thus, in the case of normal incidence of the laser radiation on a planar surface, the expression for the heat flow partial differential equation with temperature $T(x, t)$ at any time t is written in the form

$$\rho c_p \frac{\partial T(x,t)}{\partial t} = k\frac{\partial^2 T(x,t)}{\partial x^2} + \alpha I \tag{5}$$

Here $T(x, t)$ is time-dependent temperature distribution in the irradiated sample (in Kelvin), k is the thermal conductivity of the material (W/m K), ρ is the density of the material (kg/m^3), and c_p is the specific heat capacity of the material (J/kg K):

$$\text{With } \eta = \frac{k}{\rho c_p} \tag{6}$$

which is defined as the thermal diffusivity (m^2/sec), so the heat balance equation in one-dimensional case becomes

$$\frac{\partial^2 T(x,t)}{\partial x^2} = \frac{1}{\eta}\frac{\partial T(x,t)}{\partial t} - \frac{1}{\eta}\frac{\alpha I}{\rho c_p} \tag{7}$$

Eq. (7) is also called the heat diffusion equation.

In general, the heat Eq. (7) is a non-linear partial differential equation, which makes finding an analytic solution difficult. The situation is further complicated in real material systems due to changes in the optical properties (and hence the volumetric heating term) as a function of temperature and laser intensity. Thus, quantitative information generally requires methods such as finite difference and finite element numerical analysis. In some cases of extremely rapid material heating or very small material dimensions, the continuum assumptions of (7) may break down during the initial laser-material interaction requiring alternative modeling such as molecular dynamic simulations (Zhigilei et al., 1997). In certain cases, there are simplifying assumptions that can be applied to enable analytic solutions, such as treating material properties as constants, incorporating laser heating through the boundary conditions for the case of surface absorption, or treating the laser shape term as a delta function for the case of a tightly focused laser spot. Accordingly, to solve the heat diffusion equations, it is assumed that, the temperature is independent thermo-physical properties of the material. This means that, the optical absorption of the material surface and other thermal parameters such as thermal conductivity, density, and heat capacity are independent of the temperature. The solution of Eq. (7) is obtained for two different cases of absorption process as follows.

2.2.1. Case (I): Slab with surface absorption

The semi-infinite solid is a special case that is rarely found within the realm of high technology, where thin films of one kind or another are deposited on substrates (solar cells fabrication). In truth such systems can be composed of many layers (photovoltaics Manufacturing), but each additional layer adds complexity to the modeling. However, treating the system as a thin film on a substrate, while perhaps not always strictly accurate, is better than treating it as a homogeneous body.

a. Times less than the pulse length ($t < \tau$)

First, the temperature $T(x, t)$ at the surface can be calculated at any value of thickness X, and time T less than the laser pulse length $\tau(t < \tau)$. So, the solution of Eq. (7) becomes

$$T(x, t<\tau) = \frac{2\alpha I_0(1-R)}{k}(\eta t)^{1/2} ierfc\left[\frac{x}{2(\eta t)^{1/2}}\right] \tag{8}$$

where the symbol *ierfc* represents the ***Integrated Error Function Complementary*** and for any variable Z, is defined as

$$ierfc(Z) = \frac{1}{\sqrt{\pi}}e^{-Z^2} - Z\ erfc\ (Z) \tag{9}$$

Putting $Z = \frac{x}{2(\eta t)^{1/2}}$, in Eq. (8), and substituting in Eq. (9), this gives

$$ierfc\left(\frac{x}{2(\eta t)^{1/2}}\right) = \frac{1}{\sqrt{\pi}}\, e^{-\left[\frac{x}{2(\eta t)^{1/2}}\right]^2} - \left(\frac{x}{2(\eta t)^{1/2}}\right) erfc\left(\frac{x}{2(\eta t)^{1/2}}\right) \tag{10}$$

Substituting Eq. (10) into Eq. (8), and with $D = (\eta t)^{1/2}$, the final formula of the temperature behavior at any times ($t < \tau$) becomes

$$T(x, t<\tau) = \frac{2\alpha I_0(1-R)}{k} D\left\{\frac{1}{\sqrt{\pi}}e^{-\left[\frac{x}{2D}\right]^2} - \left(\frac{x}{2D}\right) erfc\left(\frac{x}{2D}\right)\right\} \tag{11}$$

And the surface temperature ($x = 0$) is given as

$$T(0, t<\tau) = \frac{2\alpha I_0(1-R)}{k} D\left\{\frac{1}{\sqrt{\pi}}\right\} \tag{12}$$

b. Times greater than the pulse length ($t > \tau$)

In this case, the heat diffusion equation is solved at any time greater than the pulse length ($t > \tau$), so, the temperature profile is obtained by a linear combination of two terms, one delayed with respect to the other. This is expressed in the following formula:

Table 1 Specification of laser parameters.

Laser	Wavelength (nm)	Pulse length (τ) (ns)	Energy density (J/cm^2)	Power density (W/cm^2)
XeCl excimer	308	30	~0.4	$\sim 1.3 \times 10^7$
Q-switched Nd:YAG	1064	6	~40	$\sim 6.7 \times 10^9$

$$T(x,t>\tau)=\frac{2\alpha I_0(1-R)}{k}\left\{\begin{array}{c}(\eta t)^{1/2}ierfc\left[\frac{x}{2(\eta t)^{1/2}}\right]\\-[\eta(t-\tau)]^{1/2}ierfc\left[\frac{x}{2[\eta(t-\tau)]^{1/2}}\right]\end{array}\right\} \tag{13}$$

The difference between the two terms of Eq. (13) is equal to the pulse duration.

2.2.2. Case (II): Absorption in slab with optical penetration

It is assumed here that, the surface absorption is occurred with optical penetration. For a spatially uniform source incident on semi infinite or slab of thickness x, the closed solution to the heat transfer equations with optical penetration into the thickness gets the temperature behavior at any time t. This is written in the form (von Allmen and Blatter, 1995)

$$T(x,t)=\frac{\alpha I_0(1-R)}{k}\left\{\begin{array}{c}2(\eta t)^{1/2}ierfc\left[\frac{x}{2(\eta t)^{1/2}}\right]-\frac{1}{\alpha}e^{-\alpha x}\\+\frac{1}{2\alpha}e^{\alpha^2(\eta t)}\left[\begin{array}{c}e^{-\alpha x}erfc\left[\alpha(\eta t)^{1/2}-\frac{x}{(\eta t)^{1/2}}\right]\\+e^{\alpha x}erfc\left[\alpha(\eta t)^{1/2}+\frac{x}{(\eta t)^{1/2}}\right]\end{array}\right]\end{array}\right\} \tag{14}$$

This simple heating model tends to treat simple structures such as a semi-infinite thickness target or a slab.

3. Discussion and data analysis

The thermal model concerning the relations of the temperature evolution is applied on two different samples of the materials (Si and GaAs). Performance specifications and estimated values of laser parameters, used in this analysis, are given in Table 1. The thermal and optical properties for Si and GaAs materials, calculated at room temperature, are listed in Table 2 a and b respectively.

The computations are carried out using an estimated thickness of slab equals 1 μm (Bauhuis et al., 2004; Grandidier et al., 2012; Sheng et al., 2013; Andreani et al., 2014). This value is taken and applied for both Si and GaAs. It is notified here that, in the following figures, we consider the symbol (a) represents Silicon Si sample, and (b) GaAs sample. The obtained results are discussed in detail as follows.

3.1. Nd:YAG laser

First, the mathematical model is applied on the material samples irradiated with Q switched Nd:YAG laser with the properties given in Table 1. Fig. 1 shows the temperature profile of the slab, and its variation with depth for both Si and GaAs respectively. The figure gives the analytical solution and the heating process for the case of time less than the laser pulse duration ($t < \tau$) and surface absorption of beam energy. The heating curves are plotted from 0.12 ns (bottom) to 5.52 ns (top) with time intervals of 0.6 ns. From the figure, it is seen that, all curves are at maximum values at the surface ($x = 0$) and gradually decreased and approximately tend to be zero with depth. It is seen also that, the temperature is increased with time of heating and this is shown in Fig. 2 for all time till to the pulse duration (6 ns). This behavior is observed in the two materials used in this analysis. The difference in data (a) and (b) in these figures is considerably as a result of optical properties and absorption process for the two samples.

For the case of time greater than the pulse duration ($t > \tau$), the cooling curves representing the variation of the temperature with time and depth are plotted in Figs. 3 and 4. The temperature profile is calculated at different times up to 2τ after the end of laser pulse. It is shown from the figures that, the cooling curves decrease as the time increases especially at the surface and up to certain values of depth. While the depth is increased, and with more time up to 2τ, the temperature is propagated into the depth, and it begins to be increased with small values until the thickness L. This behavior is shown in the two samples and in small value of thickness for GaAs than that obtained for Si. This indicates the accumulation of heat

Table 2 Thermal and optical properties of the used materials.

Thermal properties	(Si)	(GaAS)
(a) Thermal properties		
ρ (kg/m^3)	2330	5320
c_p (J/kg K)	703	350
k (W/m K)	150	33
Band gap energy (eV)	1.11	1.4

Properties	XeCl excimer (308 nm)		Q-switched Nd:YAG (1064 nm)		Ref
	(Si)	(GaAS)	(Si)	(GaAS)	
(b) Optical properties					
Reflectivity R%	0.56	0.41	10	10	David Sands (2011) and Stanowski (2011)
Absorption coefficient α (cm^{-1})	1.4×10^6	0.78×10^6	10^4	30	David Sands (2011) and Mohlmann (1984)

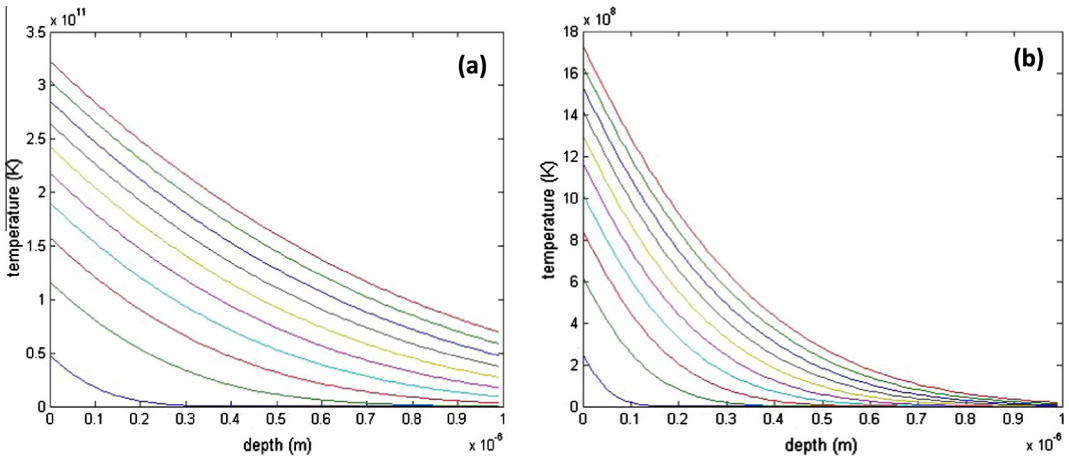

Figure 1 Surface temperature as a function of depth for the samples irradiated with Nd:YAG laser at 0.12 ns (bottom) up to 5.52 ns (top) with intervals 0.6 ns.

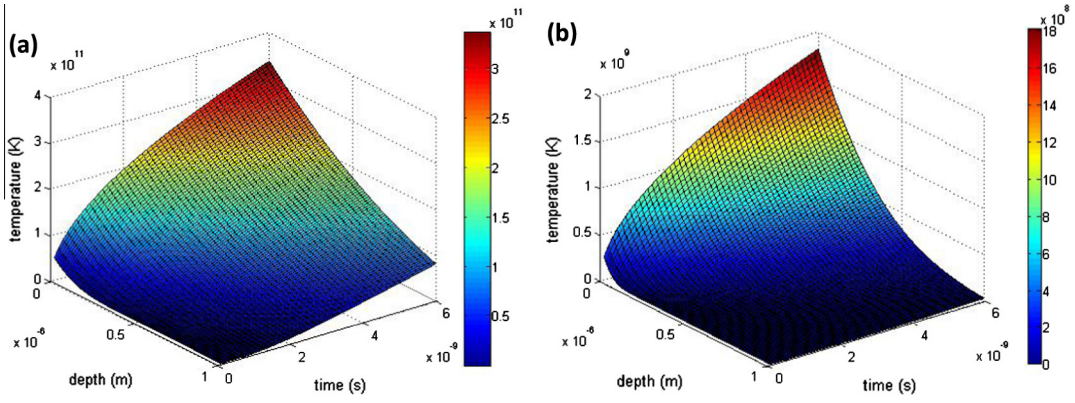

Figure 2 Surface temperature as a function of time and depth irradiated with Nd:YAG laser time intervals up to the pulse duration $\tau = 6$ ns.

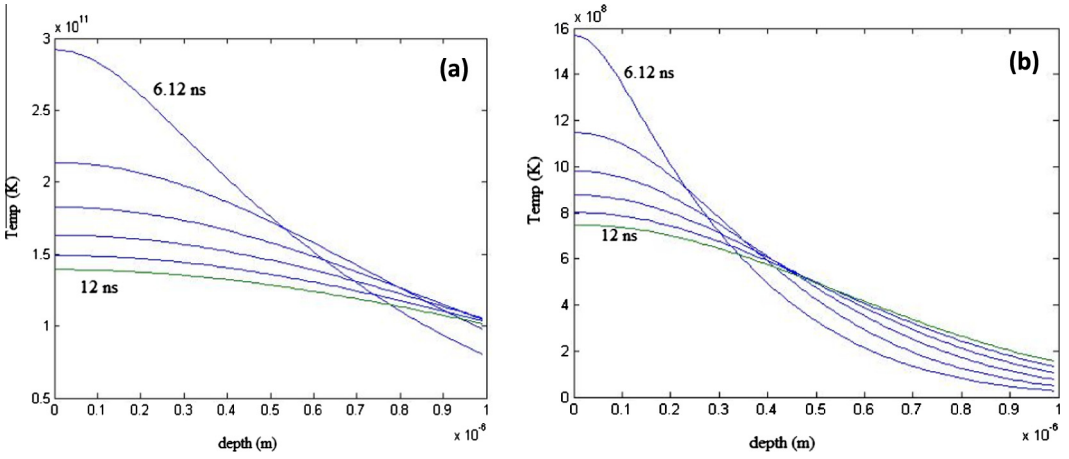

Figure 3 Cooling temperature as calculated for 6.12, 7.32, 8.52, 9.72, 10.92, and 12 ns.

within the depth is occurred as the time flows. These results agree well with those obtained in the work of Jellison et al. (1986), and David Sands (2011) and are also confirmed with those experimentally studied by Larson et al. (1983).

The temperature profiles versus depth and time are plotted at any time (as shown in Fig. 5 for ($t = 0.01\tau$), and Fig. 6 for ($t = 0.1\tau$)) as well as for time $t = \tau$ as shown in Figs. 7 and 8 respectively. From the figures, it is seen that, at a very small

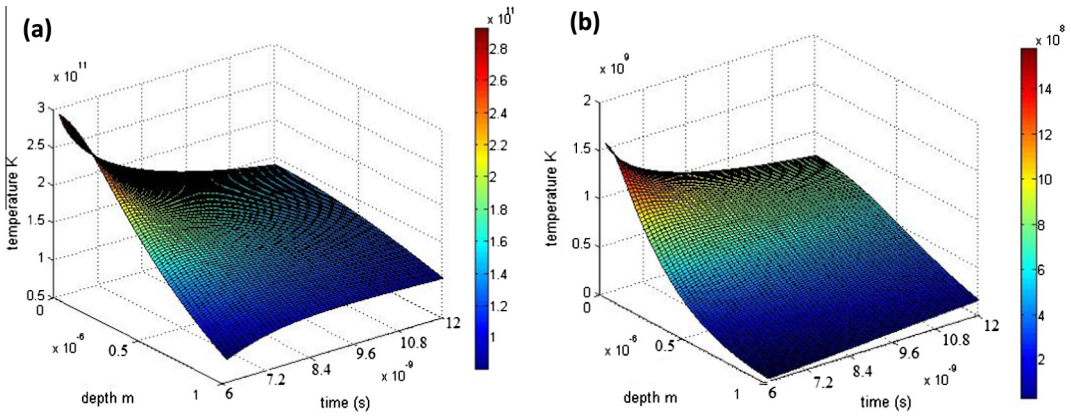

Figure 4 Cooling temperature versus the depth for all time intervals up to 2τ.

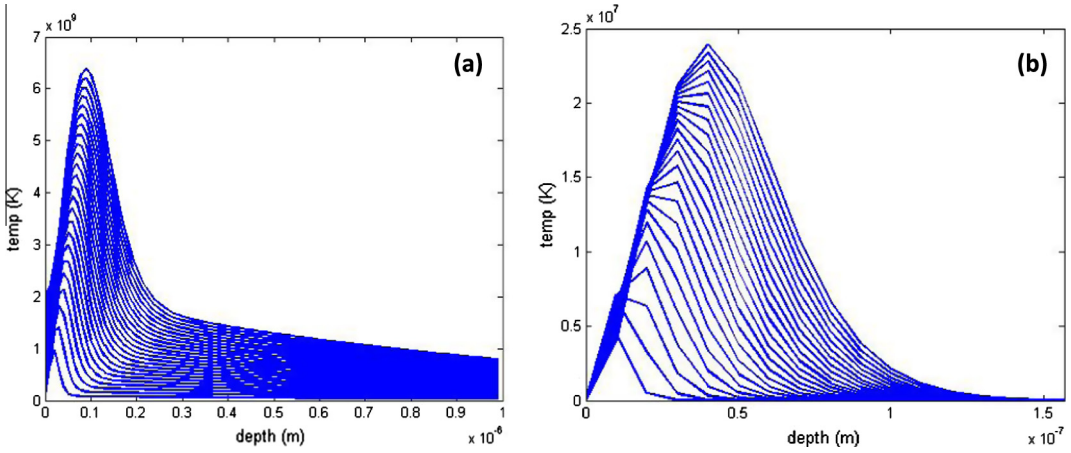

Figure 5 Temperature profiles versus depth at time $t = 0.01\tau$.

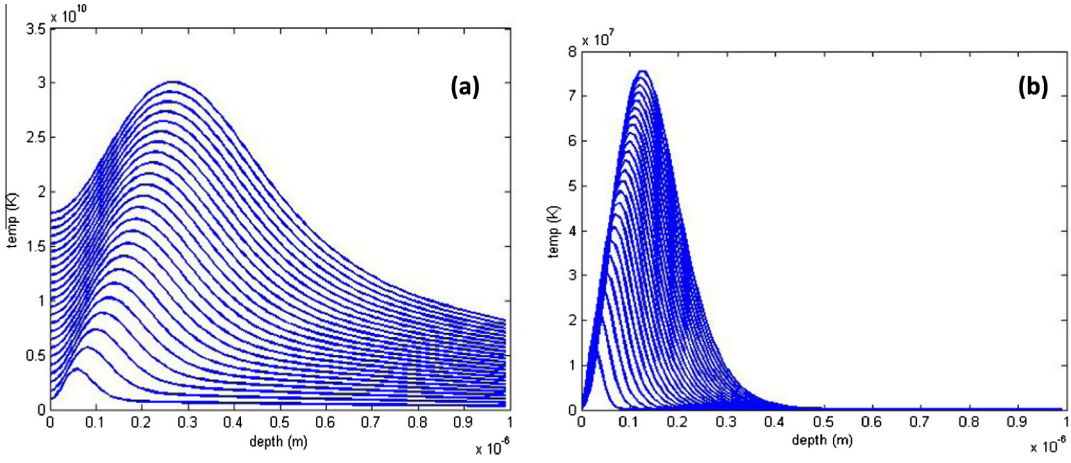

Figure 6 Temperature profile versus depth at time $t = 0.1\tau$.

time, the temperature is seen to be with the high values at a small depth close to the surface ($x = 0$). In other words, the maximum values of temperature are shown in a place still close to the surface and the peaks are increased with time till to the maximum one. With the increase in time, the temperature is increased with depth and the downhill of temperature is gradually decreased with thickness. This is due to the absorption which occurs within the depth. While the time is increased, the heat gain inside the depth overcomes on the distribution due to absorption and the temperature begins to rise to be higher in depth than on the surface. After a certain time, the heat in depth is increased leading to the accumulation which

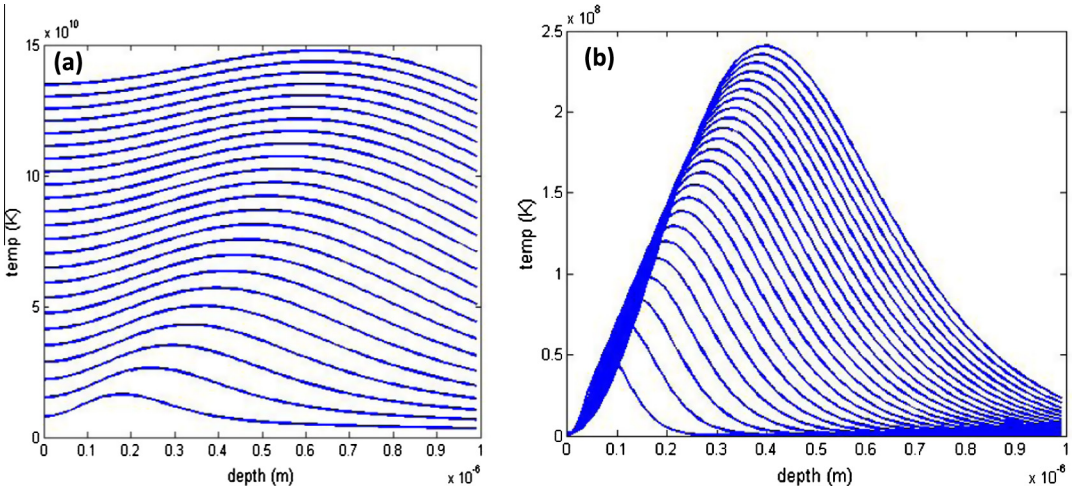

Figure 7 Temperature profile versus depth at time $t = \tau$.

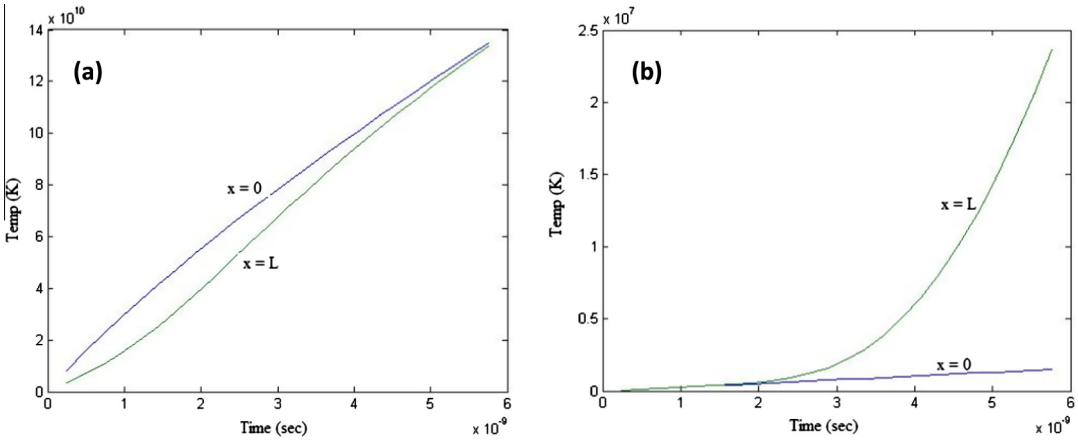

Figure 8 Temperature behavior versus time at the surface, the depth ($x = L$) till $t = \tau$.

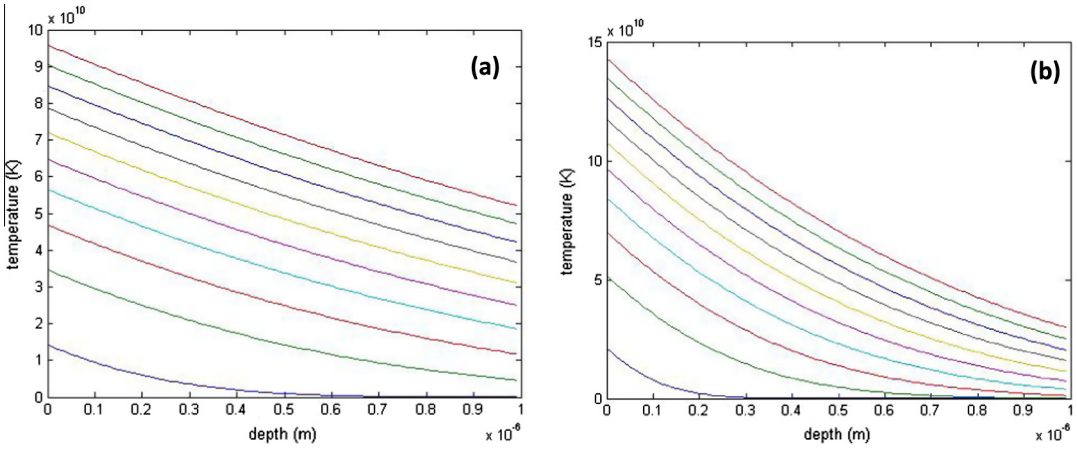

Figure 9 Surface temperature as a function of depth for the samples irradiated with XeCl excimer laser at 0.6 ns (bottom) up to 27.6 ns (top) with intervals 3 ns.

is occurred and increases in its value at the end of the depth. It is important to notify here that, for time greater than the pulse duration the temperature values are not real, in which the melting process is occurred, and the material may be damaged. This behavior is comparable to that obtained in the previous studies (Bovatsek et al., 2010; Yuan and Wu, 2014).

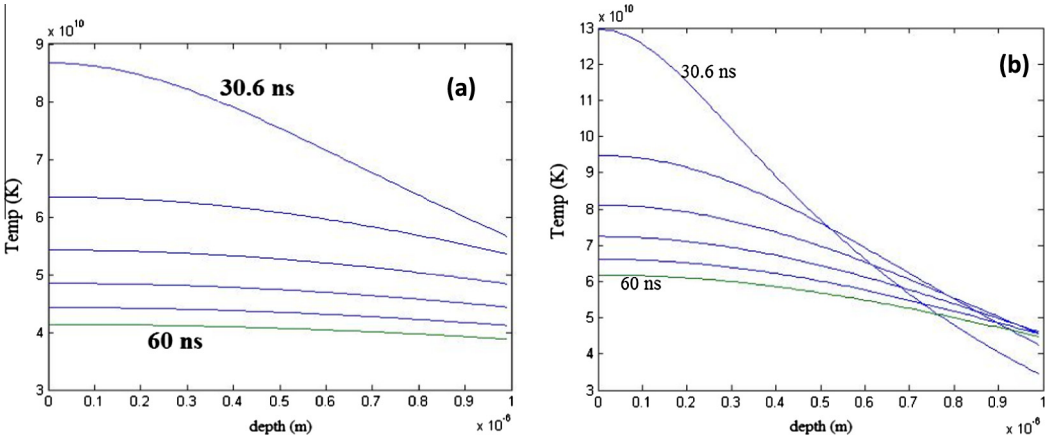

Figure 10 Cooling temperature as calculated for 30.6, 36.6, 42.6, 48.6, 54.6, and 60 ns.

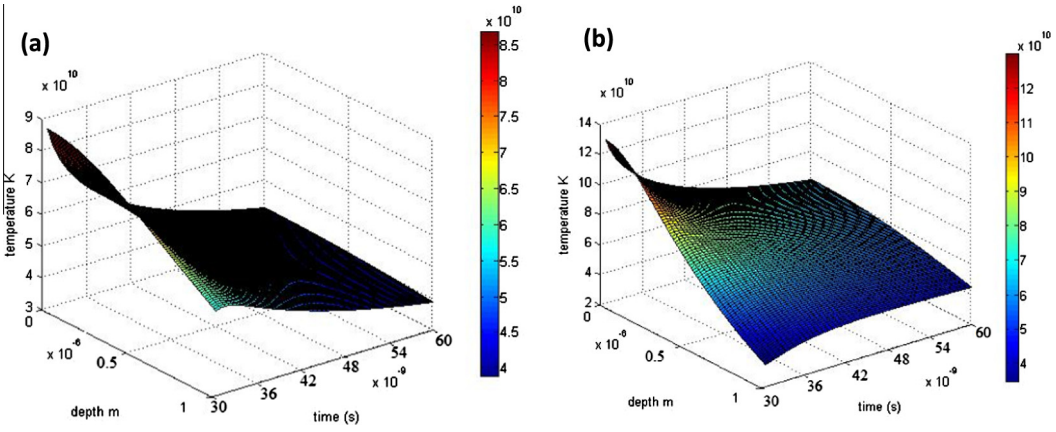

Figure 11 Cooling temperature versus the depth and all time intervals up to 2τ.

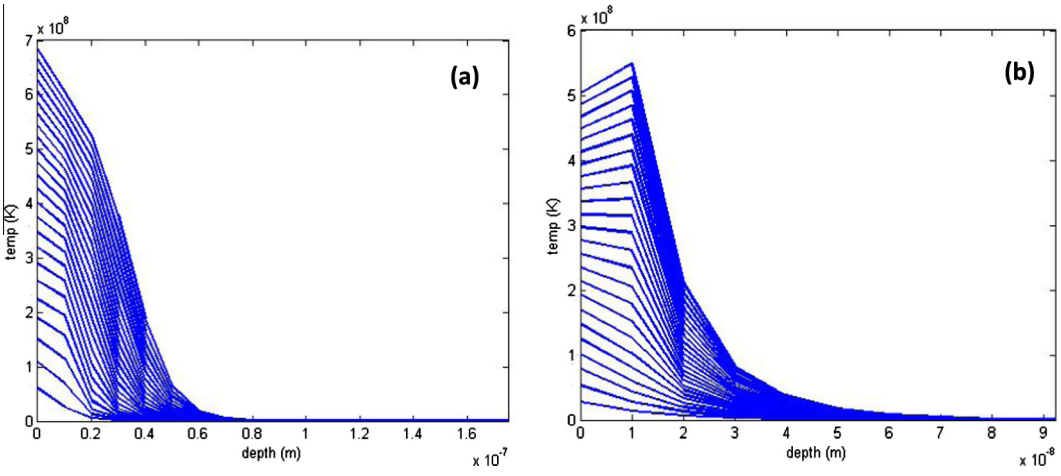

Figure 12 Temperature profile versus depth at $t = 0.0001\tau$.

3.2. XeCl excimer laser

To show the effect of the laser properties on the temperature behavior and heating process of the two samples, XeCl excimer laser with different properties is applied. The calculation is taken for the same conditions considered in case of Nd:YAG laser. This is illustrated in the following figures. It is noticed here that, the temperature is considerably still with high values up to the end of depth for both heating and cooling curves (Figs. 9–11). This is because of the different values of laser

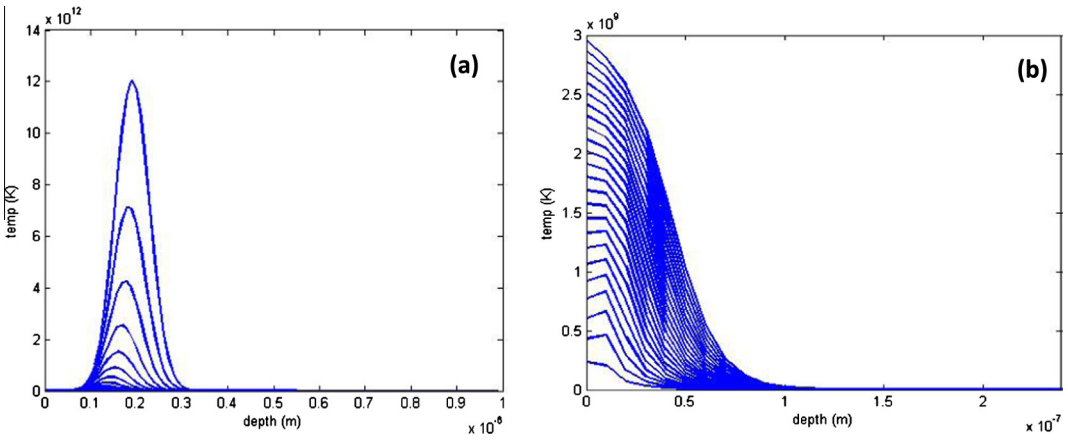

Figure 13 Temperature profiles versus depth at time $t = 0.001\tau$.

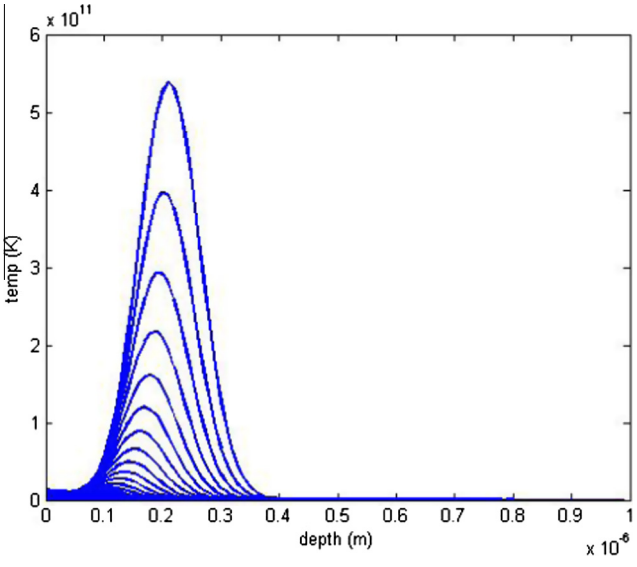

Figure 14 Temperature profile of GaAs with depth at time $t = 0.01\tau$.

intensity and pulse length. This also means the variation of optical properties (representing in optical absorption coefficient) for the materials with the laser wavelength.

With the solution of Eq. (14), the data are analyzed at any time t. The values of time are $t = 0.0001\tau$, $t = 0.001\tau$, and $t = 0.01\tau$ and are shown in Figs. 12–14 respectively. These selected values are chosen arbitrary. Above these values (i.e. as the time is increased), the data results cannot be calculated. This is strongly confirmed that the material reached to be melting and may be damaged. The temperature tends to be unreal and not realistic values and reached up to 10^{12} K for Si, and (10^{11} K) for GaAs, that is illustrated in Figs. 13a and 14 respectively.

4. Conclusion and future work

In this paper, a mathematical model of laser irradiation on samples of solar cell materials (Si and GaAs) is presented. The equations governing the temperature and heat flow diffusion through the samples are given. The thermal diffusion and heat balance equations are solved analytically at various estimated times, considering a one-dimensional heat flow and the optical radiations are absorbed at the sample. Two different types of laser light sources with different intensities and wavelengths are considered and applied in the analysis. The present model provides a prediction of the temperature elevation and the thermal response of the cell sheet/slab of two layers or more, as well as of multilayer photovoltaic cells under the effects of laser irradiation. This may be useful to optimize and outline the design of the long-range energy transmission system, especially for light-electricity systems. Moreover, this study is used to estimate the performance limits of photovoltaic receivers for laser beamed power in space in case of satellite-powered by laser illumination during eclipse and lunar night.

In the next work, the effect of pulsed laser irradiation on the considered cell samples will be experimentally studied. The threshold conditions for laser-effects (heating, melting, as well as evaporation and ablation) on the materials of cell manufacture will be examined and the experimental results will be compared with the theoretically obtained results.

References

Andreani, Lucio Claudio, Bozzola, Angelo, Kowalczewski, Piotr, Liscidini, Marco, 2014. Photonic structures for light trapping in thin-film silicon solar cells. 29th EUPVSEC, Amsterdam, Nanophotonics Workshop, 24-09.

Bauhuis, G.J., Schermer, J.J., Mulder, P., Voncken, M.M.A.J., Larsen, P.K., 2004. Thin film GaAs solar cells with increased quantum efficiency due to light reflection. Sol. Energy Mater. Sol. Cells 83, 81–90.

Bovatsek, J., Tamhankar, A., Patel, R.S., Bulgakova, N.M., Bonse, J., 2010. Thin film removal mechanisms in ns-laser processing of photovoltaic materials. Thin Solid Films 518, 2897–2904.

Brown, Matthew S., Arnold, Craig B., 2010. Fundamentals of laser-material interaction and application to multiscale surface modification. In: Sugioka, K. et al. (Eds.), . In: Laser Precision Microfabrication, Springer Series in Materials Science, vol. 135. Springer-Verlag, Berlin Heidelberg. http://dx.doi.org/10.1007/978-3-642-10523-4_4 (Ch. 4).

Cuce, Erdem, Cuce, Pinar Mert, Bali, Tulin, 2013. An experimental analysis of illumination intensity and temperature dependency of photovoltaic cell parameters. Appl. Energy 111, 374–382.

David Sands, 2011. Pulsed laser heating and melting. In: Prof. Vyacheslav Vikhrenko (Ed.), Heat Transfer – Engineering Applications. ISBN: 978-953-307-361-3.

Flournoy, D.M., 2012. What is a solar power satellite. In: Pelton, J.N. (Ed.), Solar Power Satellite. Springer, New York, pp. 1–8.

Grandidier, Jonathan, Callahan, Dennis M., Munday, Jeremy N., Atwater, Harry A., 2012. Gallium arsenide solar cell absorption enhancement using whispering gallery modes of dielectric nanospheres. IEEE J. Photovolt. 2, 2.

Green, M.A., 1998. Efficiency limits, losses, and measurement. In: Holonyak, N., Jr.Jr. (Ed.), Solar Cells: Operating Principles, Technology, and System Applications. University of New South Wales, Sydney, pp. 85–102.

Green, M.A., Emery, K., Hishikawa, Y., Warta, W., 2011. Solar cell efficiency tables, (version 37). Prog. Photovoltaics Res. Appl. 19, 84–92.

Jellison Jr., G.E., Lowrides, D.H., Wood, R.F., 1986. Fundamental aspects of pulsed-laser irradiation of semiconductors. In: Proceedings of the Society of Photo-Optical Instrumentation Engineers September 14–26, Cambridge, MA.

King, R.R., Law, D.C., Edmondson, K.M., et al, 2007. 40% efficient metamorphic GaInP/GaInAs/Ge multi-junction solar cells. Appl. Phys. Lett. 90, 183516.

Kuanr, A.V., Bansal, S.K., Srivastava, G.P., 1996. Laser-induced damage in InSb at 1.06 pm wavelength – a comparative study with Ge, Si and GaAs. Opt. Laser Technol. 28, 345–353.

Landis, Geoffrey A., 1991a. Photovoltaic Receivers for Laser Beamed Power in Space. NASA Contractor Report 189075, December 1991.

Landis, G.A., 1991b. Satellite eclipse power by laser illumination. Acta Astronaut. 25, 229–233.

Larson, B.C., White, C.W., Noggle, T.S., Barhorst, J.F., Mills, D.M., 1983. Appl. Phys. Lett. 42, 282.

Laudani, Antonino, Mancilla-David, Fernando, Riganti-Fulginei, Francesco, Salvini, Alessandro, 2013. Reduced-form of the photovoltaic five-parameter model for efficient computation of parameters. Sol. Energy 97, 122–127.

Mohlmann, G.R., 1984. Neutral and ionic particle emission produced by laser irradiation of a GaAs surface. J. Laser Chem. 5, 1–10.

Raikunov, G.G., Mel'nikov, V.M., Chebotarev, A.S., et al, 2011. Orbital solar power stations as a promising way for solving energy and environmental problems. Therm. Eng. 58, 917–923.

Schafer, C.A., Gray, D., 2012. Transmission media appropriate laser-microwave solar power satellite system. Acta Astronaut. 79, 140–156.

Sheng, Xing et al, 2013. Doubling the power output of bifacial thin-film GaAs solar cells by embedding them in luminescent waveguides. Adv. Energy Mater. 3, 991–996.

Shuvalov, V.A., Kochuojoj, G.S., Prejjmak, A.E., 2002. Electrical properties changes of solar panel under space environment. Space, Sci. Technol. 8, 25–36.

Stanowski, R.W., 2011. Nano-engineering band gap quantum semi conductors rapid thermal annealing laser. PhD Thesis.

Von Allmen, M., Blatter, A., 1995. Laser-Beam Interactions with Materials: Physical Principles and Applications. Springer Series in Materials Science. Springer, Berlin.

Yuan, Yu-chen, Wu, Chen-wu, 2014. Thermal response of photovoltaic cell to laser beam irradiation. In: Proceedings for "The Heat Transfer Symposium", Beijing, China, May 6–9.

Yuan, Yu-chen, Wu, Chen-wu, Chen, Guangnan, 2013. Responses of thin film photovoltaic cell to irradiation under double laser beams of different wavelength. Mater. Sci. Forum 743–744, 937–942.

Zhigilei, L.V., Kodali, P.B.S., Garrison, B.J., 1997. J. Phys. Chem. B 101 (11), 2028.